# Geotechnical Assessment of the Slopes of Hamamok Dam, NE of Koya, Kurdistan Region of Iraq

Bahra Dh. Ghafour[1*], Mohammed J. Hamawandy[1], and Varoujan K. Sissakian[2]

[1]Department of Geotechnical Engineering, Faculty of Engineering, Koya University,
Koya KOY45, Kurdistan Region - F.R. Iraq

[2]Department of Petroleum Engineering, Komar University of Science and Technology,
Sulaymaniyah, Kurdistan Region – F.R. Iraq

***Abstract*—The Hamamok Dam is an earthfill dam with a height of 25 m and a length of 125 m, constructed in 2011, located northwest of Koya town on a deep canyon-like valley that flows along the southeastern plunge of the Bana Bawi anticline, which forms Bawagi Mountain. The exposed rocks at the site belong to the Pila Spi and Gercus Formations; however, rocks from the Khurmala and Kolosh formations are exposed upstream from the dam's reservoir. The difference in the hardness of the carbonate rocks of the Pila Spi formation, which forms the uppermost parts of the cliffs surrounding the dam site, and those of the soft reddish brown clastics of the Gercus Formation caused steep slopes that suffered from slope instability problems. To perform a geotechnical study of slopes at the dam site, we have collected different field data to perform a kinematic assessment method using DipAnalyst 2.0 software and drawn the stereographic projections for the studied 10 stations using Stereonet v11 software. Besides, Bejerman's method, which is based on field data, is used to indicate the landslide possibility index (LPI). The results showed that the LPI values range between 23 and 27, whereas the results of the kinematic analysis showed that the right bank (stations 1–5) suffers from plane sliding, whereas the left bank (stations 6–10) suffers from toppling. In both cases, Joint 2 has the main role in the developed failures.**

***Index Terms*—Bejerman's method, Factor of safety, Hamamok Dam, Kinematic analysis, Landslide possibility index.**

## I. Introduction

The Ministry of Agricultural and Water Resources in the Kurdistan Regional Government has planned to construct tens of dams of different sizes at different places in the Kurdistan Region of Iraq. Among those dams is the Hamamok Dam, it is an earth fill dam, constructed in 2011 with a height of 25 m, a length of 120 m, and a reservoir capacity of 250,000 m$^3$. The dam is constructed on a deeply incised valley that flows along the southeastern plunge of the Bana Bawi anticline, and it is represented by Bawagi Mountain, which is the western continuation of the Haibat Sultan Range Fig. 1.

ARO-The Scientific Journal of Koya University
Vol. XII, No. 1 (2024), Article ID: ARO.11553. 10 pages
DOI: 10.14500/aro.11553
Received: 25 February 2024; Accepted: 25 May 2024
Regular research paper: Published: 17 June 2024
Corresponding author's e-mail: bahra.dhahir@koyauniversity.org


## II. Hamamok Dam

Hamamok Dam is an earthfill dam with a length of 120 m, and a height of 25 m, and the surface area of the lake at an elevation of about 800 m (a.s.l.) is 18,044 m$^2$. Both upstream and downstream sides are paved by limestone blocks up to 0.3 m$^3$ as rip-rap, and the spillway is built on the right side of the dam at an elevation of 803 m (a.s.l.). On the left and right banks of the dam and the lake, and more upstream and downstream sides very steep slopes and cliffs are developed, and the slopes suffer from different types of failures.

The slope failures are developed due to the existence of the soft clastic rocks of the Gercus Formation overlain by hard carbonate rocks of the Pila Spi Formation (Sissakian and Fouad, 2014). The average gradients of the left and right banks of the lake are 53.51% and 23.62%, respectively. Whereas, the maximum heights on the left and right banks of the lake are 1300 m and 950 m, respectively, Fig. 2.

## III. Geological Setting

Hamamok Dam is located in the High Folded Zone. It is a part of the Zagros-Fold-Thrust Belt (Fouad, 2015). The dam is constructed in a deep valley that flows along the southeastern plunge of the Bana Bawi anticline and a few hundred meters west of the Koisanjaq syncline Fig. 1. The northwestern hanging plunge of the Koisanjaq syncline forms an elevated area; called Bawaji Mountain. Some of the carbonate rocks of the Pila Spi Formation show microfolding with an amplitude of (1–5) m. These micro folds have accelerated the deformation of the beds and their break down into small pieces, accordingly, increasing the slope failure phenomenon. Both abutments of the dam are constructed within the clastic rocks of the Gercus Formation (Eocene age), which consists of reddish-brown fine clastics; mainly claystone and sandstone. In general, the beds are soft forming steep slopes. The thickness of the formation is about 80 m. The Gercus Formation is overlain by the Pila Spi Formation

http://dx.doi.org/10.14500/aro.11553

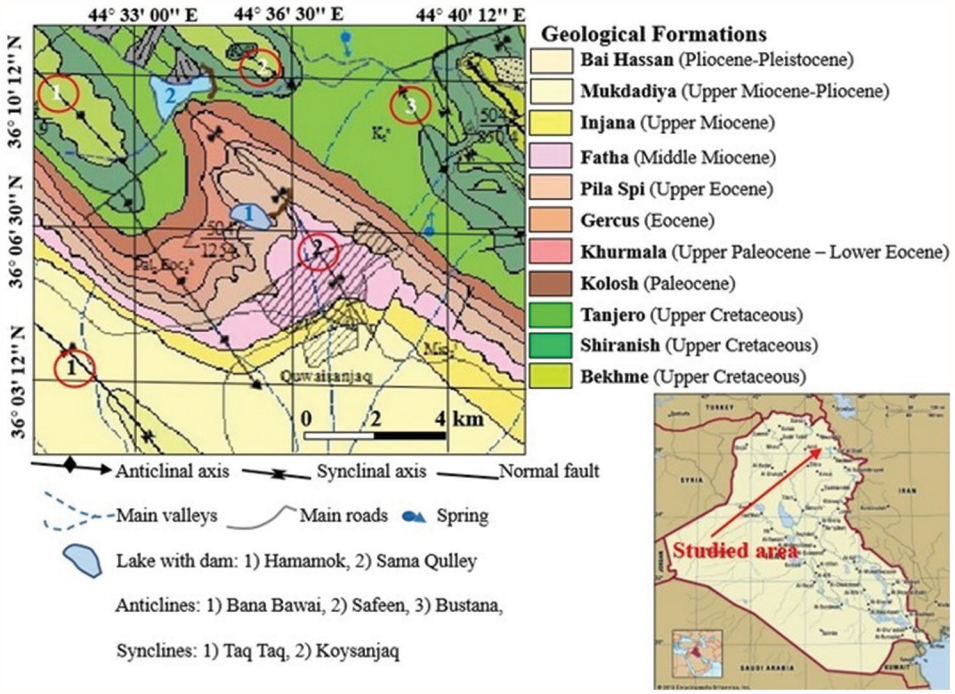


Fig. 1. Location and geological map of Hamamok Dam and surroundings, modified from (Sissakian and Fouad, 2014).

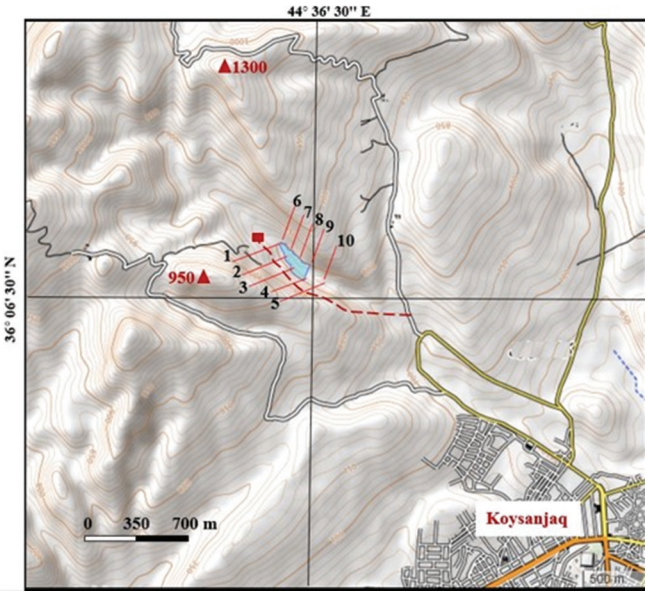


Fig. 2. Contour map of the studied area with the location of the studied 10 stations. The approximate coordinates, scale, and the unpaved road to the dam site (red dashed line) and guard house (red rectangle) are added by the authors after (Inkatlas, 2023).

(Upper Eocene age) Fig. 1. It consists of hard to very hard limestone and dolostone, and cliff-forming. The thickness of the formation is about 60 m (Sissakian and Fouad, 2014).

The most well-developed geomorphological form in the studied area is the giant flat irons Fig. 3. The average values of the width, height, and elevation difference between the top and bottom are 1.8 km, 1.3 km, and 305 m, respectively.

The steep slopes and cliffs are also well-developed at the dam site. These are attributed to the soft clastic rocks of the Gercus Formation, which are overlain by hard carbonate rocks of the Pila Spi Formation Fig. 3.

## IV. Methodology and Work Procedure

We have reviewed many published scientific articles, which dealt with (Bejerman, 1994) and Kinematic analysis for geotechnical assessment of slope stability. We also used a geological map at a scale of 1:250,000 (Sissakian and Fouad, 2014; Esriimage, 2023; Inkatlas, 2023) to find relevant data relevant to Hamamok Dam site. For the geotechnical assessment of the slopes around the Hamamok Dam and the lake, we used two different methods, (1) the (Bejerman, 1994) Method, and (2) the Kinematic Method using DipAnalyst 2.0 software, and drawing the stereographic projection for the 10 studied stations using Stereonet v11 software.

We have used both methods because (1) Bejerman's Method is a quick and easy field method without the need for special laboratories, equipment, and specialized personnel, (2) We have used the Kinematic Method based on data from an abandoned tunnel, which is near the dam site, and (3) No field sampling and rock coring equipment is available.

### *A. Bejerman Method*

This is a simple and quick field method through which any artificial or natural slope can be assessed geotechnically (Bejerman, 1994), (Bejerman, 1988). The method depends on 10 attributes Fig. 4. All can be measured and/or estimated in the field directly. Therefore, it is a very quick method.

We have selected 10 stations (five on each side of the dam site and reservoir) (Fig. 2) to represent the stability status on the slopes of both sides, each station is opposite to the other

one on the other side. Moreover, the last station on each side (numbers 5 and 10) is on the downstream of the dam. This was done to indicate the difference in the stability of the slopes upstream and downstream sides.

The height of the slope was measured from the Google Earth image. The slope angle and gradient of discontinuities were measured using Ferrybridge Compass. The grade of weathering, fracture, gradient of discontinuities, vegetation cover, and existing landslides were estimated directly in the field by personal observation. The spacing of discontinuities was measured using measuring tape. The orientation of discontinuities was indicated based on the dip direction of the rocks and the slope direction. The water infiltration was indicated directly in the field based on the presence of water among the slopes and the type of rocks.

### *B. Kinematic Analysis*

The Kinematic analysis is the second analysis method, which we applied to assess the slopes of the Hamamok Dam site. This method is used to analyze the potential for the different modes of rock slope failures (plane, wedge, and toppling failures), which take place due to the presence of discontinuities that have unfavorable orientations. We found it to be a kind of block failure through the stereonet. The direction in which the block will slide can be detected using the same diagram; moreover, the stability condition can be detected (Goodman, 1976; Hoek and Bray, 1977; Wyllie and Mah, 2005). The software used was DipAnalyst 2.0, which is designed for both new quantitative kinematic analysis and stereonet-based analysis. To determine whether a dip direction or value has the potential to cause a plane or toppling failure, the software compares it with the slope angle and friction angle. There is a chance of a plane failure if the dip vector (middle point of the great circle) of the great circle, which represents a discontinuity set, lies inside the shaded region where the friction angle is greater than the slope angle. However, if the dip vector (the great circle's midpoint) falls inside the triangle-shaped shaded area, there is a chance that the structure will topple over.

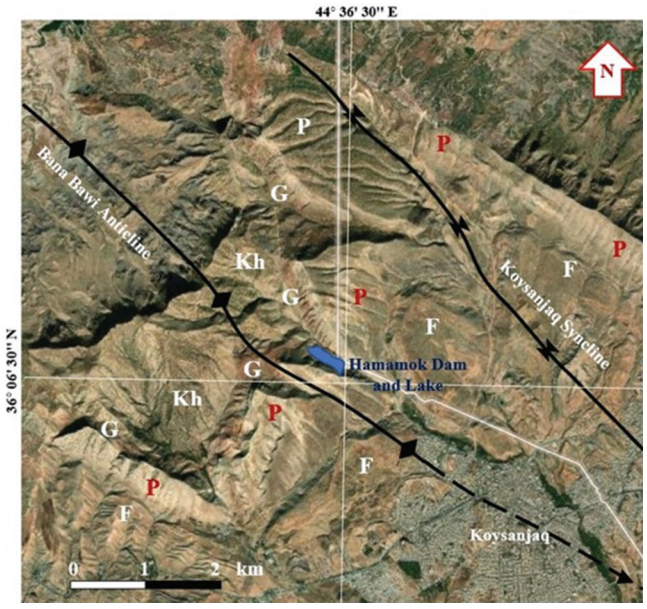


Fig. 3. Giant flat irons on the southeastern plunge of the Bana Bawi Anticline and Koysanjaq Syncline. Geological Formations: Kh=Khurmala, G=Gercus, P=Pila Spi, and F=Fatha (Esriimage, 2023).

## V. Results

### *A. Bejerman Method*

The obtained field data for (Bejerman, 1994) Method Table I were used to indicate the grade, category of the landslide possibility index (LPI) and hazard zones. The results are shown in Table II; based on (Bejerman, 1994) Method Table III. The obtained LPI values showed that the Category ranges between High (7 stations) and Very high (3 stations). Hazard zones range between Moderate (8 stations) and High (2 stations), whereas the Failure possibility ranges between High (8 stations) and Very high (2 stations).

### *B. Kinematic Analysis*

The stereographic projections and Dip analysis 2.0 diagrams are presented in (Figs. 4 and 5) for the right and left banks' stations, respectively. By DipAnalyst 2.0 software the factor of safety can be calculated for plane and wedge failure but we cannot obtain it for toppling failure. Therefore, the values of the factor of safety were obtained only for stations 1, 2, 3, 4, and 5, which are presented in Table IV. The values of Friction angle, Cohesion and rock density were acquired from the geotechnical study of the Haibat Sultan tunnel (Bosphorus Technical Consulting Corporation, 2012), which is located about 1.5 km east of the study area within the same rocks and same geological condition (Sissakian and Fouad, 2014). Whereas, the results of the Kinematic analysis of the studied 10 stations using Dip analysis 2.0 are presented in (Tables V and VI).

For all stations, in stereographic (Figs. 4 and 5) (1B, 2B, 3B, 4B, 5B, 6B, 7B, 8B, 9B, and 10B), the slope face with the daylight window (envelope) and two lateral limit lines are in blue. Joint 2 is pink in color, joint1 is in orange color, the bedding plane is brown and the internal friction angle is in green color. For Dip Analyst (Figs. 4 and 5) (1A, 2A, 3A, 4A, 5A, 6A, 7A, 8A, 9A, and 10A), the slope face is in red and joints 1 and 2 are in orange and pink color, respectively. The bedding plane is in brown and the internal friction angle is in green color, whereas the critical area is determined by the Dip Analyst software.

## VI. Discussion

### *A. Bejerman's Method*

The high values of LPI and failure possibilities in the banks of the Hamamok Dam site (Tables III and IV) indicate that the slopes on both banks are unstable (Figs. 6 and 7). The unstable slopes are attributed to: (1) the Steep slopes of both banks of the valley, which form the lake of the dam (Fig. 2) have gradients of 53.51% and 23.62% of the left and right banks, respectively, (2) the well bedded and jointed hard carbonate rocks of the

Pila Spi Formation, which suffer from toppling (Figs. 6 and 7), (3) the presence of soft claystone beds of the Gercus Formation underlying the carbonate rocks of the Pilea Spi Formation act as a lubricant for sliding and toppling, and (4) the high rates of weathering and erosion in the site.

*B. Kinematic Analysis*

Based on (Markland, 1972; Hocking, 1976; Hoek and Bray, 1981; Wyllie and Mah, 2005) the modes of failure are analyzed. A potentially unstable planar block needs to meet the following conditions in order to occur:

- The bedding plane, which is referred to as a "daylight" on the face, dips at a flatter angle than the slope face ($\psi A < \psi f$)
- Considering that every discontinuity strikes nearly parallel to the slope face, the poles of the slope face and the discontinuity sets (symbol P) are plotted on the stereonet and displayed in (Figs. 4 and 5). These poles' positions with respect to the slope face demonstrate that all planes' poles are daylight, potentially unstable and located inside the slope face's pole. The daylight envelope, also known as the "Daylight Window," is this region that can be used to rapidly identify blocks that may be unstable
- -The stability will also be impacted by the discontinuity sets' dip direction. Only when the discontinuity's dip direction and the slope face's dip direction diverge by <20ϕ, or $|\alpha A - \alpha f| < 20\phi$, can plane sliding be achieved. In stations Nos. 1, 2, 3, 4, and 5 (Fig. 4), this is the situation, and Joint 2 plays a major part in the plane siding
- Two lines (Slope limits in the plane) defining the dip directions of ($\alpha f + 20\ \phi$) and ($\alpha f - 20\ \upsilon$) on the stereonet illustrate this restriction on the dip direction of the planes. The lateral boundaries of the daylight envelope in (Fig. 9) are indicated by these two lines.

Goodman and Bray (1976) and Wyllie and Mah (2005) state that the following conditions must be met for toppling failure to occur:

- In order to form a series of slabs parallel to the slope face, the discontinuities dipping into it must have a dip direction that is within approximately 10¸ of the slope face's dip direction. Two lines (Slope limits in the plane) that define the dip directions of ($\alpha f + 10\acute{r}$) and ($\alpha f - 10\acute{r}$) on the stereonet illustrate this restriction on the dip direction of the planes. The lateral boundaries of the daylight envelope in (Fig. 8) are indicated by these two lines. As shown in Fig. 6, this

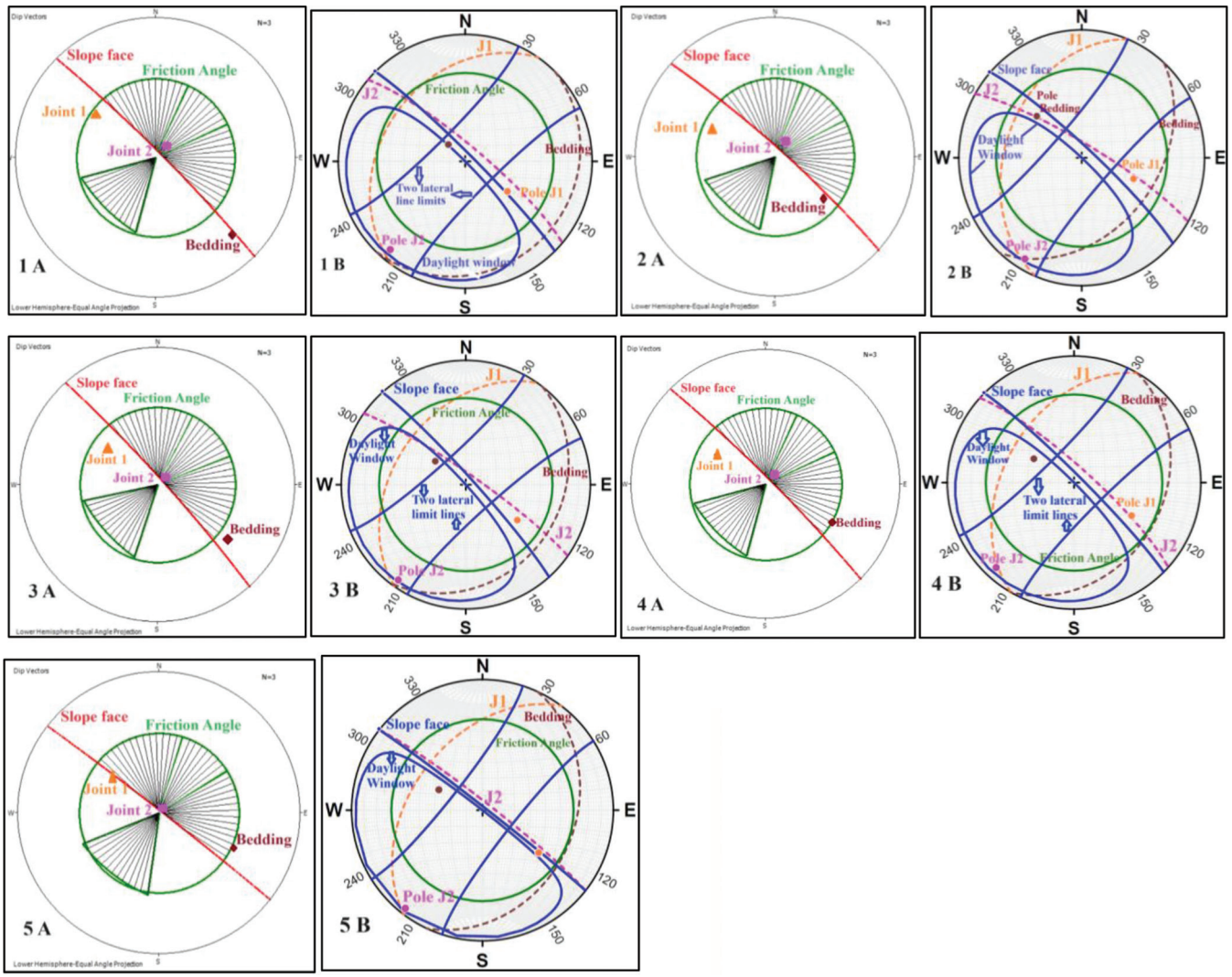


Fig. 4. Stereographic projections and Dip analysis diagrams of stations 1, 2, 3, 4, and 5 of the Hamamok Dam.

http://dx.doi.org/10.14500/aro.11553

TABLE I
FIELD DATA OF THE 10 STUDIED STATIONS AT THE HAMAMOK DAM SITE

| Station No. | Numbers of the attributes used in LPI from (Bejerman, 1994) | | | | | | | | | | Rating LPI | Coordinates | | Elevation (m, a.s.l.) | Figure No. in the text |
|---|---|---|---|---|---|---|---|---|---|---|---|---|---|---|---|
| | 1 | 2 | 3 | 4 | 5 | 6 | 7 | 8 | 9 | 10 | | | | | |
| | Slope | | Grade of | | Discontinuities | | | Vegetation cover (%) | Water infiltration (%) | Previous land slide volume | | | | | |
| | Height (m) | Angle (°) | Fracture | Weathering | Gradient (°) | Spacing (m) | Orientation | | | | | Latitude (N) | Longitude (E) | | |
| 1 | 121 | 85 | H | H | 34 | 0.3–1.0 | Unf | Void | Inexist | High | 24 | 36°06.183' | 44°35.847' | 840 | 7.1 |
| | 5 | 4 | 2 | 3 | 2 | 2 | 4 | 0 | 0 | 2 | | | | | |
| 2 | 125 | 83 | H | H | 38 | 0.3–1.0 | Unf. | Scarce | Inexist. | High | 25 | 36°06.143' | 44°35.183' | 838 | 7.2 |
| | 5 | 4 | 2 | 3 | 2 | 2 | 4 | 1 | 0 | 2 | | | | | |
| 3 | 110 | 85 | H | H | 62 | 0.3–1.0 | Unf | Scrace | Inexist | H | 27 | 36°06.100' | 44°35.957' | 828 | 7.3 |
| | 5 | 4 | 2 | 3 | 4 | 2 | 4 | 1 | 0 | 2 | | | | | |
| 4 | 72 | 85 | H | H | 44 | 0.3–1.0 | Unf | Scrace | Inexist | H | 25 | 36°06.079' | 44°36.146' | 815 | 7.4 |
| | 5 | 4 | 2 | 3 | 2 | 2 | 4 | 1 | 0 | 2 | | | | | |
| 5 | 70 | 88 | H | H | 45 | 0.3–1.0 | Unf | Void | Inexist | Small | 24 | 36°06.137' | 44°36.037' | 824 | 7.5 |
| | 5 | 4 | 2 | 3 | 3 | 2 | 4 | 0 | 0 | 1 | | | | | |
| 6 | 141 | 60 | H | H | 55 | 0.3–1.0 | Unf | Void | Inexist | Small | 23 | 36°06.140' | 44°35.183' | 830 | 8.6 |
| | 5 | 3 | 2 | 3 | 3 | 2 | 4 | 0 | 0 | 1 | | | | | |
| 7 | 98 | 65 | H | H | 50 | 1–3 | Unf | Void | Inexist | Small | 23 | 36° 06. 142' | 44°35.180' | 822 | 8.7 |
| | 5 | 4 | 2 | 3 | 3 | 1 | 4 | 0 | 0 | 1 | | | | | |
| 8 | 87 | 80 | H | H | 62 | 0.3–1.0 | Unf | Void | Inexist | High | 26 | 36°06.140' | 44°35.957' | 810 | 8.8 |
| | 5 | 4 | 2 | 3 | 4 | 2 | 4 | 0 | 0 | 2 | | | | | |
| 9 | 72 | 82 | H | H | 64 | 0.3–1.0 | Unf | Void | Inexist | Small | 25 | 36°06.137' | 44°36.037' | 784 | 8.9 |
| | 5 | 4 | 2 | 3 | 4 | 2 | 4 | 0 | 0 | 1 | | | | | |
| 10 | 68 | 85 | H | H | 57 | 0.3–1.0 | Unf | Void | Inexist | High | 25 | 36°06.135' | 44°36.041' | 824 | 8.10 |
| | 5 | 4 | 2 | 3 | 3 | 2 | 4 | 0 | 0 | 2 | | | | | |

LPI: Landslide possibility index

http://dx.doi.org/10.14500/aro.11553

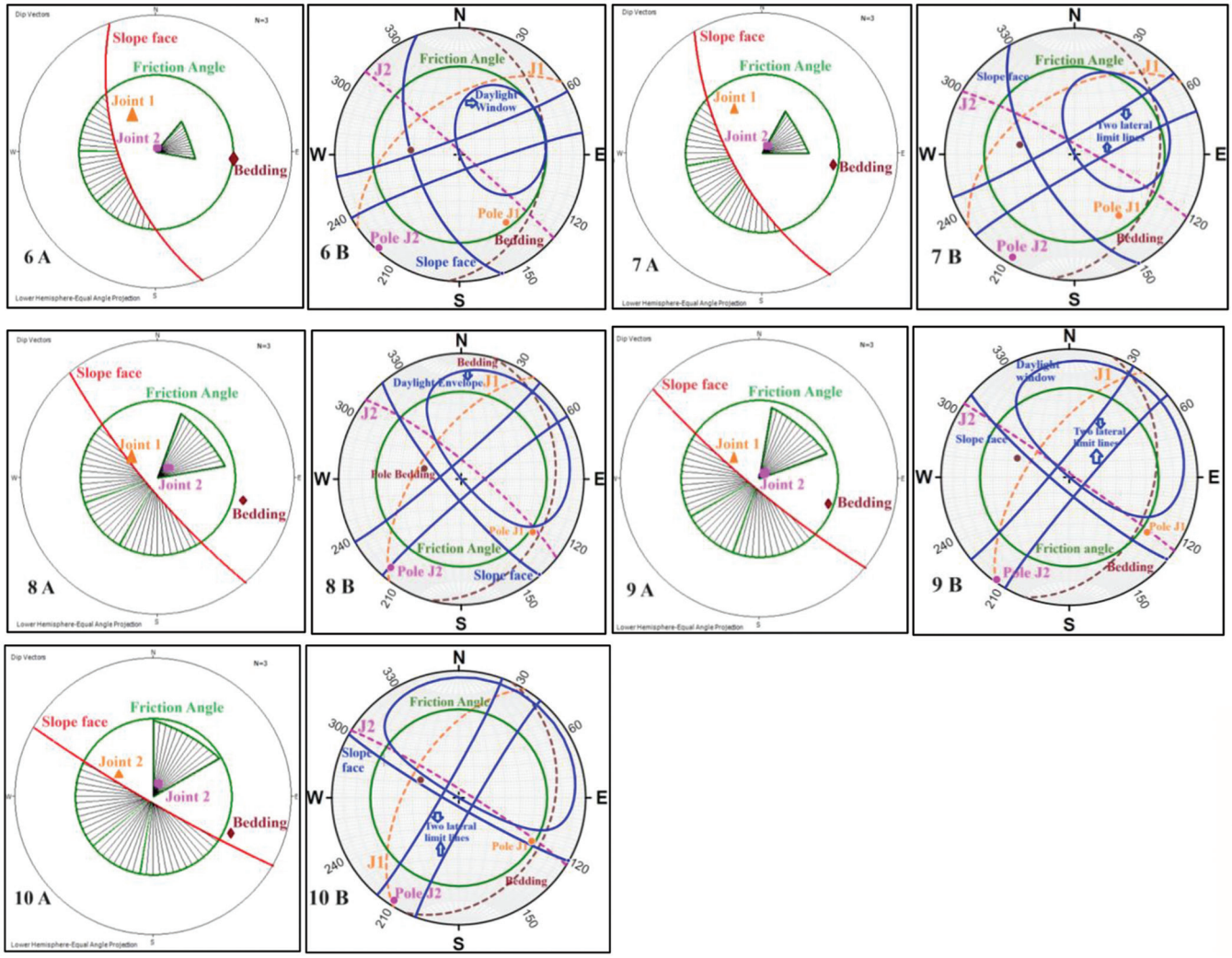


Fig. 5. Stereographic projections and Dip analysis diagrams of stations 6, 7, 8, 9, and 10 of the Hamamok Dam.

TABLE II
LPI Scored Values, Hazard Zones and Failure Possibility (After Bejerman, 1994) at 10 Stations

| Station No. | LPI Value | LPI | | Hazard Zone | Failure possibility |
|---|---|---|---|---|---|
| | | Grade | Category | | |
| 1 | 24 | V | High | Moderate | High |
| 2 | 25 | V | High | Moderate | High |
| 3 | 27 | VI | Very High | High Hazard | Very High |
| 4 | 25 | V | High | Moderate | High |
| 5 | 24 | V | High | Moderate | High |
| 6 | 23 | V | High | Moderate | High |
| 7 | 23 | V | High | Moderate | High |
| 8 | 26 | VI | Very High | High Hazard | Very High |
| 9 | 25 | V | High | Moderate | High |
| 10 | 25 | V | High | Moderate | High |

LPI: Landslide possibility index

TABLE III
Landslides Hazard Categories, Hazard Zones, and Failure Possibility Range after (Bejerman, 1994; Bejerman, 1998)

| Landslide possibility index (LPI) | | | Hazard Zone | | Failure possibility | |
|---|---|---|---|---|---|---|
| Grade | Category | Estimation | | | | |
| I | Small | 0–5 | <10 | Low hazard | 0–5 | Small |
| II | Very Low | 6–10 | | | 6–10 | Very Low |
| III | Low | 11–15 | 11–25 | Moderate hazard | 11–15 | Low |
| IV | Moderate | 16–20 | | | 16–20 | Moderate |
| V | High | 21–25 | <25 | High hazard | 20–25 | High |
| VI | Very High | <25 | | | >25 | Very High |

is the situation at stations Nos. 6, 7, 8, 9, and 10. Joint 2 is primarily responsible for the toppling.

- The planes' dip needs to be sufficiently steep for interlayer slip to happen. Slip will only happen if the direction of the applied compressive stress is at an angle larger than ϕj with a normal direction to the layers if the friction angle on the layers' faces is ϕj. When the following circumstances are met, interlayer slip and toppling failure will occur on planes with dip ψp, as the major principal stress in the cut is oriented parallel to the cut face (dip angle ψf) (Goodman and Bray, 1976).
- The dip of the planes must be steep enough for interlayer slip to occur. If the faces of the layers have a friction angle ϕj, then slip will only occur if the direction of the

TABLE IV
NUMERICAL USED DATA IN THE CALCULATION OF THE FACTOR OF SAFETY.

| Station No. | Slope face (Direction/ Inclination amount) | Discontinuity Dip direction/Dip amount | Slope height (m) | Cohesion ($Kn/m^2$) | Friction Angle (°) | Rock Density ($Kn/m^3$) | Tension Cracks (Depth/ height of water) (cm) | Factor of safety |
|---|---|---|---|---|---|---|---|---|
| 1 | 045/85 | 040/80 | 121 | 61 | 31 | 25 | 50/2 | 0.57 |
| 2 | 042/83 | 030/81 | 125 | 61 | 31 | 25 | 60/4 | 0.97 |
| 3 | 048/85 | 035/83 | 110 | 61 | 31 | 25 | 65/4 | 0.99 |
| 4 | 045/85 | 042/80 | 72 | 61 | 31 | 25 | 55/3 | 0.89 |
| 5 | 038/88 | 038/85 | 70 | 61 | 31 | 25 | 50/3 | 0.64 |

TABLE V
RESULTS OF KINEMATIC ANALYSIS OF THE 5 STUDIED STATIONS ON THE RIGHT BANK SLOPE OF THE HAMAMOK DAM

| Station No. | Kinematic analysis | | DipAnalyst 2.0 software and Stereographic projection results |
|---|---|---|---|
| | Angles relationship between Joint 2 and Slope face ($\psi A<\psi f$) | Relation between the direction of discontinuities and slope face $\lvert\alpha A-\alpha f\rvert <20^\circ$ | |
| 1 | The dip of joint 2 and its relation with the slope angle has a minor to moderate effect on the sliding failure because there is almost less difference between them. (80° <85°). | The dip direction of Joint 2 has a main role in sliding as the difference in their direction to the direction of the slope face is <20°. \|310–315\|=5 <20° | The stereographic projection for this station shows that the friction angle is greater than the slope angle and pole of the Joint 2 lies in the critical area for planar failure (between two lateral limit lines on the edge of the daylight window area) Fig. 5. 1B. The analysis by Dip Analysis 2.0 shows that the dip vector point of Joint 2 lies within the critical area for plane sliding criteria Fig. 5. 1A and the numerical analysis by DipAnalyst 2.0 software shows that the value of the factor of safety is 0.57 Table IV. Therefore, the potentiality for plane sliding is high. |
| 2 | The slope angle is almost equal to the dip of Joint 2, thus it has a minor to moderate effect on sliding failure in this station. (81° <83°) | The direction of Joint 2 has a significant role in sliding as the difference in their direction to the direction of the slope face is <20°. \|300–312\|=12 <20° | As is clear in Fig. 5. 2B the friction angle is greater than the slope angle, and the pole of Joint 2 lies within a critical area (between two lateral limit lines in the daylight window area). For DipAnalyst 2.0 software, the analysis shows that there is a medium possibility for sliding by joint 2 which lies on the edge of the critical zone for plane sliding Fig. 5. 2A. The numerical analysis by DipAnalyst 2.0 software shows that the value of the factor of safety for this station is 0.97 Table IV which indicates that the possibility of sliding failure is low. |
| 3 | The dip of the slope is almost equal to the dip of Joint 2, thus it has a minor to moderate effect on sliding failure in this station. (83°<85°) | Joint 2 has a significant role in sliding failure in this station as the difference of its direction to the direction of the slope face is <20°. \|305–318\|=13 <20 | At this station, Joint 2 has the main effect on sliding failure as it is clear in (Fig. 5. 3B) that its pole lies on the edge of the line of the critical area between two lateral limits planes of the daylight window zone for sliding failure. The Analysis by DipAnalyst 2.0 software shows that the probability for sliding failures on the Joint 2 surfaces is potential as it lies within the critical area (Fig. 5. 3A). Therefore, the potentiality of plane sliding exists. The factor of safety for this station is 0.99 (Table IV) therefore the sliding possibility is low. |
| 4 | The dip of joint 2 and its relation with the slope angle has a minor to moderate effect on the sliding failure because there is almost less difference between them. (80° <85°) | In this station, the difference between the dip direction of Joint 2 and the slope face is<20o. Thus it has a main role in sliding failure\|312–315\|=3<20 | (Fig. 5. 4B) shows that joint 2 has the main effect on sliding failure where it lies within a critical area between two slope limit planes in the daylight window zone. (Fig. 5. 4A) for The DipAnalyst 2.0 software shows that Joint 2 lies on the edge within the critical plane sliding zone. Therefore, the type of failure in this station is plane sliding. Numerical Analysis by DipAnalyst 2.0 software shows that the value of the factor of safety for this station is 0.89 (Table IV). |
| 5 | The dip of joint 2 and its relation with the slope angle has a minor to moderate effect on the sliding failure because there is almost less difference between them. (85° <88°) | The dip direction of Joint 2 has a main role in sliding as the difference in their direction to the direction of the slope face is <20°. \|307–308\|=1 <20 | At this station, joint 2 has the main effect on sliding failure as it's clear in (Fig. 5. 5B) its pole lies within the area between two lateral slope limits planes of the daylight window zone (critical area) for sliding failures. (Fig. 5. 5A) for analysis by DipAnalyst 2.0 software shows that the probability for sliding failures on the Joint 2 surfaces is high, as it lies within the critical area zone for plane sliding failure. Numerical analysis shows that the factor of safety for this station is 0.64 (Table IV). Therefore, the potentiality of plane sliding is high. |

applied compressive stress is at an angle greater than $\phi j$ with a normal direction to the layers. The direction of the major principal stress in the cut is parallel to the face of the cut (dip angle $\psi f$), so interlayer slip and toppling failure will occur on planes with dip $\psi p$; when the following conditions are met (Goodman and Bray, 1976):

http://dx.doi.org/10.14500/aro.11553


Fig. 6. Right bank station Nos. 1, 2, 3, 4, and 5. Nos. 1 and 4: Active erosion areas indicating unstable slopes. No. 2: Bulged mass in the middle of the slope indicating an unstable slope. No. 3: Recent slid blocks as indicated from the fresh color of the blocks; indicating unstable slope. No. 5: The slope below the cliff is gentler as compared to the other stations; therefore, the amount of slid blocks is smaller and lesser. The reddish brown clastics of the Gercus Formation are overlain by the carbonates of the Pila Spi formation

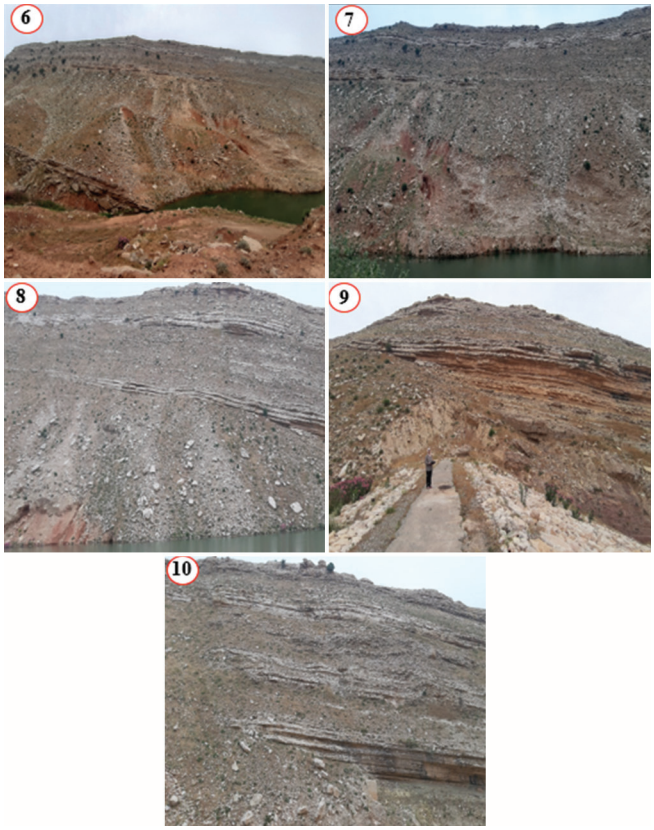


Fig. 7: Left bank station Nos., 6, 7, 8, 9, and 10. Nos. 6, 7, and 8: Active erosion areas and groves within the slopes indicating unstable slopes. No. 9: Bulged mass on the left of the slope indicating unstable slope. No. 10: Microfolds in the beds of the Pila Spi Formation, they deformed the beds and increased the instability of the slopes. Note the amount of the accumulated scree in the left side of the slope. The reddish brown clastics of the Gercus Formation are overlain by the carbonates of the Pila Spi Formation.

TABLE VII
The Attitude of Bedding Planes, Joints, ( 1 and 2), and Slope Face in the Hamamok Dam Site

| Station | | Bedding plane | | | Joint No. 1 | | | Joint No. 2 | | | Slope face | | |
|---|---|---|---|---|---|---|---|---|---|---|---|---|---|
| No. | Location | Strike (°) | Dip (°) | | Strike (°) | Dip (°) | | Strike (°) | Dip (°) | | Strike (°) | Inclination Dip (°) | |
| | | | Direction | Angle | | Direction | Angle | | Direction | Angle | | Direction | Angle |
| 1 | Right Bank | N 45 E | 135 | 15 | N 35 E | 305 | 34 | N 50 W | 40 | 80 | 315 | 45 | 85 |
| 2 | | N 42 E | 132 | 40 | N 22 E | 292 | 38 | N 60 W | 30 | 81 | 312 | 42 | 83 |
| 3 | | N 32 E | 128 | 25 | N 35 E | 305 | 42 | N 55 W | 35 | 83 | 318 | 48 | 85 |
| 4 | | N 30 E | 120 | 30 | N 30 E | 300 | 44 | N 48 W | 42 | 80 | 315 | 45 | 85 |
| 5 | | N 25 E | 115 | 30 | N 37 E | 307 | 45 | N 53 W | 38 | 85 | 308 | 38 | 88 |
| 6 | Left Bank | N 05 E | 95 | 32 | N 53 E | 325 | 55 | N 49 W | 41 | 88 | 340 | 250 | 60 |
| 7 | | N 10 E | 100 | 35 | N 55 E | 325 | 50 | N 60 W | 30 | 84 | 330 | 240 | 65 |
| 8 | | N 15 E | 105 | 25 | N 36 E | 306 | 62 | N 51 W | 39 | 80 | 320 | 230 | 80 |
| 9 | | N 20 E | 110 | 35 | N 35 E | 305 | 64 | N 62 W | 28 | 88 | 310 | 220 | 82 |
| 10 | | N 25 E | 115 | 27 | N 31 E | 301 | 57 | N 58 W | 32 | 85 | 300 | 210 | 85 |

**$(90°–\psi f)+\phi j<\psi p$**

To perform the Dip analysis 2.0, the strike and dip direction of the exposed beds and existing joint sets at each station were measured, besides the direction and inclination amount of the slope face. The results are presented in (Table VII). The data of rock properties from (Bosphorus Technical Consulting Corporation, 2012), which belongs to an abandoned tunnel that is 1.2 km east of the dam site and dug within the same rocks (the Pila Spi Formation) were adopted. The adopted data include (1) static friction angle, (2) rock density, and (3) cohesion for the construction of the stereonet projections, the adopted data are shown in (Table IV). To illustrate the relation

TABLE VI
RESULTS OF KINEMATIC ANALYSIS OF THE 5 STUDIED STATIONS ON THE LEFT BANK OF THE HAMAMOK DAM

| Station | Kinematic analysis | Stereographic and Dip analysis 2.0 projection results |
|---|---|---|
| 6 | -The Kinematic analysis in this station shows that the dip direction of Joint 2 is about N41°E dipping into the slope face (S70°W) and for toppling failure to occur it must be within about 10°, but in this station is more than 10° where the pole of Joint 2 lies outside the critical area (Fig. 5. 6B). - Numerical analysis by (Goodman and Bray, 1976): *(90°– ψf) + φj < ψp* (90–60)+31 <88=(61 <88) indicates that the potentiality of toppling failure is high. | The stereo net's slope stability analysis in (Fig. 6. 6B) shows that the pole of Joint 2 lies outside of the critical area (Daylight window) area. The analysis by DipAnalyst 2.0 software shows that Joint 2, lies on the edge of the shaded area Fig. 6. 6A). Therefore, toppling failure is possible and is increased by the activity of differential weathering and/or erosion of the claystone layer that underwent various degrees of weathering and/or erosion inward for the claystone slope face with a decrease in bearing capacity toward the slope. |
| 7 | -The Kinematic analysis in this station shows that the dip direction of joint 2 is about N30° E dipping into the slope face (S60°W) and for toppling failure to occur it must be within about 10°, but in this station is more than10°. -According to numerical analysis by (Goodman and Bray, 1976). (90-65)+31 <84=(56 <84) | Slope stability analysis by Stereo nets (Fig, 6. 7B) indicates that the toppling failure possibility is low by Joint 2 as the pole of joint 2 lies outside the critical area (Daylight window). The analysis by DipAnalyst 2.0 software shows that Joint 2, lies on the edge of the shaded area (Fig. 6. 7A). This means that the possibility for toppling failure is low because the activity of differential weathering and/or erosion of rock masses below the slopes leads to gradation in weathering, the blocks move gradually and then topple. |
| 8 | The Kinematic analysis in this station shows that the dip direction of joint 2 is about N39°E dipping into the slope face (S50°W) and for toppling failure to occur it must be within about 10°, but in this station, it is <10° and as it is clear in (Fig. 5. 8B) the pole of Joint 2 lies in the critical area (between two lateral limit lines within the daylight envelope area). Therefore, the potentiality of toppling failure is high. - According to equation analysis. (90-80)+31 <80=(41 <80) | The stereographic projection in this station (Fig. 6. 8B) shows that the possibility of toppling failure is high where the pole of Joint 2 lies in the critical area (Daylight window) on the edge of the two lateral limit lines for toppling failure. This means the blocks in this station are more prone to toppling failure than sliding where the pole of Joint 2 is far and out of the sliding failure criteria. The analysis by DipAnalyst 2.0 software shows that Joint 2, lies on the edge of the shaded area (Fig. 6. 8A), where toppling failure is possible and is increased by the activity of differential weathering and/or erosion of rock masses below the slopes. |
| 9 | The Kinematic analysis shows that the dip direction of joint 2 has a main effect on toppling failure to occur in this station as it is about N28°E dipping into the slope face (S40°W) within about 10°. -Numerical analysis according to equations by (Goodman and Bray, 1976) shows that (90-82)+31=88=(39<88) Therefore, in this station potentiality of toppling failure is high. | The stereo net's slope stability calculation for station 9 (Fig. 6. 9B) shows that the possibility for toppling failure in this station is high, where the pole of Joint 2 lies inside the critical area (Daylight window) and between the two lateral limit lines. This means that blocks in this station are more prone to toppling failure than sliding where the pole of joint 2 is far and out of the sliding failure criteria. The analysis by DipAnalyst 2.0 software shows that Joint 2, lies within the triangular shaded area (area for toppling failure) (Fig. 6. 9A) |
| 10 | The Kinematic analysis shows that the attitude of joint 2 has a main effect on toppling failure to occur in this station as it is about N32°E dipping into the slope face has attitude (S30°W) within about 10°. - According to equation analysis (90-85)+31=85=(36<85). Therefore, the potentiality of toppling failure is almost high. | The stereographic analysis for this station (Fig. 6. 10B) shows that the possibility of Toppling failure is high, where the pole of joint 2 lies inside the critical area (Daylight window) This means the blocks in this station are more prone to toppling failure than sliding where the pole of Joint 2 is far and out of the sliding failure criteria. The analysis by DipAnalyst 2.0 software shows that Joint 2, lies on the edge of the triangular shaded area (Figure 6. 10A), where toppling failure is possible. |

between the slope face direction and the orientation (dip and strike) of the joints and bedding planes of the exposed rocks at all 10 stations, stereographic projections were constructed by Stereonet v11 software.

## VII. Conclusions

To evaluate the stability of the banks of the Hamamok Dam site, two methods have been applied. Bejerman's Method, based on 10 attributes, which were measured and/or estimated directly in the field. The results showed that the LPI values range between 23 and 27, which means High to Very high failure possibility. The second method is the Kinematic method; based on DipAnalyst 2.0 software, and drawing the stereographic projection using Stereonet v11 software showed that the right bank (Stations 1–5) suffers from plane sliding, whereas the left bank (Stations 6–10) suffers from toppling. In both banks, Joint 2 has the main role in the developed unstable slopes. This is attributed to its strike direction and dip amount.

## VIII. Recommendations

Based on the acquired data on the stability of both banks and landslide possibility and their type, and because the hard carbonate rocks of the Pila Spi Formation form the top slope part, the main reasons for the possible failure are the orientation and dip amount of the bedding and joint planes; therefore, the protection measures which can be recommended are: (1) Digging a ditch on the top slope and line it by concrete to decrease the infiltration of rainwater to the rocks, (2) the ditch will also decrease the infiltrated water to the soft red claystone, which will form as a lubricant to the overlying hard carbonate rocks of the Pila Spi Formation, (3) to increase

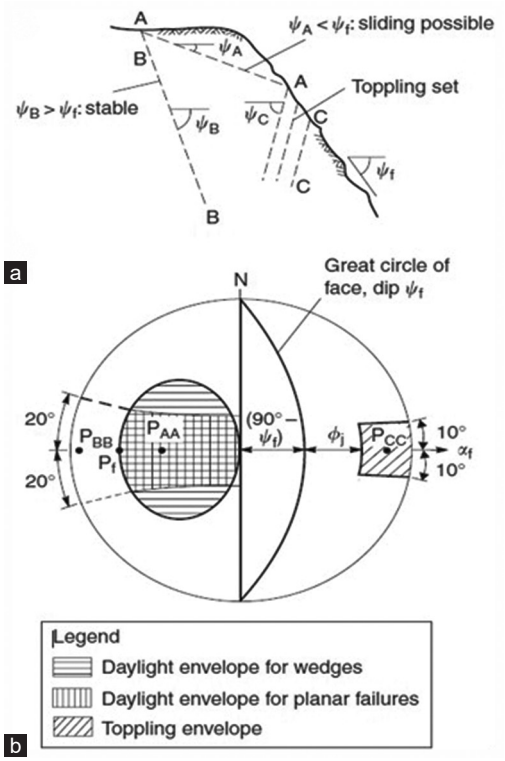


Fig. 8. Kinematic analysis of blocks of rock in slope: (a) discontinuity sets in slope; and (b) daylight envelopes on equal area stereonet.

the vegetation cover on the slopes of red soft rocks of the Gercus Formation to decrease the weathering and erosion of the soft clastic rocks which accelerate the toppling and sliding of the hard carbonate rocks, and (4) although we could not recognize very large blocks on the top slope, a detailed check should be done to check if such blocks exist or otherwise. If yes, then bolting to the bedrock should be done.

## References


Bejerman, N., 1994. Landslide Possibility Index System. In: *7th International Congress International Association of Engineering Geology*. Balkema, Rotterdam, pp.1303-1306.

Bejerman, N.J., 1988. Evaluation of Landslide Susceptibility along a Sector of State Road E-5. In: *8th International Congress of IAEG*. Vancouver, Canada, Balkima, Rotterdam.

Bosphorus Technical Consulting Corporation, 2012. (*Bosphorus Technical Consulting and Corporation*) *Design of Haibat Sultan Tunnel and Approach Roads Report*. The Ministry of Housing and Constructions, Erbil, Iraq.

Esriimage, 2023. Available from: https://earthexplorer.usgs.gov [Last accessed on 2023 Jun 05].

Fouad, S.F.A., 2015. Tectonic Map of Iraq, Scale 1: 1000000. *Iraqi Bulletin of Geology and Mining,* 11(1), pp.1-8.

Goodman, R.E., 1976. *Methods of Geological Engineering in Discontinuous Rocks.* West Publishing Co., St.Paul.

Goodman, R.E., and Bray, J., 1976. Toppling of Rock Slopes. In: *Proceedings of the Specialty Conference on Rock Engineering for Foundations and Slopes*. ASCE, pp.201-234.

Hocking, G., 1976. Amethod for distinguishing between single and double plane sliding of tetrahedral wedges. *International Journal of Rock Mechanics and Mining Sciences*, 13, pp.225-226.

Hoek, E., and Bray, J., 1977. *Rock Slope Enginering.* 1st ed., IMM, London.

Hoek, E., and Bray, J., 1981. *Rock Slope Engineering.* 3rd ed., Institution of Mining and Metallurgy, London, UK.

Inkatlas, 2023. *Inkatlas.* Available from: https://inkatlas.com/create [Last accessed on 2023 Jun 04].

Markland, J., 1972. *A Useful Technique for Estimating the Stability of Rock Slopes when the Rigid Wedge Slide Type of Failure is Expected*. Imperial College Rock Mechanics Research Report No 19.

Sissakian, V.K., and Fouad, S.F., 2014. *The Geology of Erbil and Mahabad quadrangles, scale 1:250,000*. Iraq Geological Survey Publications, Baghdad, Iraq.

Sissakian, V.K., Ghafur, A.A., Ibrahem, F.I., Abdulhaq, H.A., Hamoodi, D.A., and Omer, H.O., 2022. Suitability of the carbonate rocks of the bekhme formation for cement industry, Hareer Mountain, North Iraq, Kurdistan Region. *Iraqi Geological Journal*, 54(2c), pp.59-67.

Sissakian, V.K., Hamoudi, D.A., Omer, H.O., and Niazi, S.A., 2019. Assessment of the carbonate rocks of the Pila Spi formation for cement industry, in Permam Mountain, Erbil, Iraqi Kurdistan Region. *UKH Journal of Science and Engineering*, 3(1), pp.1-9.

Wyllie, D., and Mah, C., 2005. In: Hoek, E., and Bray, J.W., editors. *Rock Slope Engineering: Civil and Mining*. 4th ed., Spon Press, Taylor and Francis Group, London, New York.